

## Magnetic properties of Co- and Mn-implanted BaTiO<sub>3</sub>, SrTiO<sub>3</sub> and KTaO<sub>3</sub>

J.S. Lee<sup>a</sup>, Z.G. Khim<sup>a</sup>, Y.D. Park<sup>a</sup>, D.P. Norton<sup>b,\*</sup>, N.A. Theodoropoulou<sup>c</sup>,  
A.F. Hebard<sup>c</sup>, J.D. Budai<sup>d</sup>, L.A. Boatner<sup>d</sup>, S.J. Pearton<sup>b</sup>, R.G. Wilson<sup>e</sup>

<sup>a</sup> School of Physics, Seoul National University, Seoul 151-747, South Korea

<sup>b</sup> Department of Materials Science and Engineering, University of Florida, Gainesville, FL 32611, USA

<sup>c</sup> Department of Physics, University of Florida, Gainesville, FL 32611, USA

<sup>d</sup> Oak Ridge National Laboratory, Oak Ridge, TN 37831, USA

<sup>e</sup> Consultant, Stevenson Ranch, CA 91381, USA

Received 17 August 2002; received in revised form 1 September 2002; accepted 12 November 2002

### Abstract

Implantation of Co or Mn into single-crystal BaTiO<sub>3</sub>(K), SrTiO<sub>3</sub> or KTaO<sub>3</sub>(Ca), followed by annealing at 700 °C, produced ferromagnetic behavior over a broad range of transition metal concentrations. For BaTiO<sub>3</sub>, both Co and Mn implantation produced magnetic ordering temperatures near 300 K with coercivities  $\leq 70$  Oe. The  $M-T$  plots showed either a near-linear decrease of magnetization with increasing temperature for Co and a non-Brillouin shaped curve for Mn. No secondary phases were detected by high-resolution X-ray diffraction. The same basic trends were observed for both SrTiO<sub>3</sub> and KTaO<sub>3</sub>, with the exception that at high Mn concentrations ( $\sim 5$  at.%) the SrTiO<sub>3</sub> was no longer ferromagnetic. Our results are consistent with recent reports of room temperature ferromagnetism in other perovskite systems (e.g. LaBaMnO<sub>3</sub>) and theoretical predictions for transition metal doping of BaTiO<sub>3</sub> [Nakayama et al., Jap. J. Appl. Phys. 40 (2001) L1355].

© 2003 Elsevier Ltd. All rights reserved.

### 1. Introduction

Progress in growth of thin film oxide perovskite materials led to the discovery of a large negative magnetoresistance (MR) at room temperature in doped magnate perovskites [1–6]. This large MR effect is commonly referred to as colossal magnetoresistance [1]. The resistivity of materials is found to a maximum around the Curie temperature [6]. These materials have potential for magnetic sensing applications. Other families of complex oxides are attractive for a broad range of applications including UV photonics, transparent electronics, gate dielectrics on semiconductors and novel device concepts using correlated electron systems in

which charge or spin can be manipulated via electric-field gating.

An emerging field of interest is that of spintronics in which the spin of the electron rather than its charge would carry the information of interest [7,8]. Dilute magnetic semiconductors such as GaMnAs, GaMnP and GaMnN have shown rapid progress in recent years, with the latter two displaying signature of ferromagnetism above room temperature [9–13]. In addition, transparent ferromagnetic ZnMnO [14], ZnCoO [15] and TiCoO<sub>2</sub> [16,17] have all been reported and doping with other transition metal impurities is predicted to be effective in stabilizing the ferromagnetic state [18–20]. Very little work has been carried out on oxide perovskite materials, although there is a prediction that BaTiO<sub>3</sub> doped with Mn, Cr or Fe will be promising candidates for ferromagnetism [21]. MR of a number of other ZnO and SnO<sub>2</sub> films doped with various impurities have also been reported [22–26], while all perovskite oxide

\* Corresponding author. Tel.: +1-352-846-0525; fax: +1-352-846-1182.

E-mail address: [dnort@mse.ufl.edu](mailto:dnort@mse.ufl.edu) (D.P. Norton).

film p–n junctions with room temperature ferromagnetism have been demonstrated [27].

In this paper we report on investigation of the effects of direct Co and Mn ion implantation into bulk BaTiO<sub>3</sub>, SrTiO<sub>3</sub> and KTaO<sub>3</sub> single crystals. In each case we observe signatures of ferromagnetism at or near room temperature. These results show the promise of semiconducting oxides for potential spintronic applications and the flexibility of ion implantation as a method for introducing a wide variety of transition metal impurities into host materials for purposes of measuring their magnetic properties.

## 2. Experimental

Bulk, single crystal BaTiO<sub>3</sub> (K), SrTiO<sub>3</sub> or KTaO<sub>3</sub>(Ca) were implanted at ~350 °C with 250 keV Co<sup>+</sup> or Mn<sup>+</sup> ions at doses of 3 or 5 × 10<sup>16</sup> cm<sup>-2</sup>, producing incorporation depths of ~2000 Å and an average transition metal concentrations of 3 or 5 at.%. The elevated temperature during implantation is employed to minimize the possibility of amorphization. Post-implant annealing at 700 °C for 5 min under flowing N<sub>2</sub> was used to partially repair the remaining implant damage. The samples were examined by high-resolution X-ray diffraction (XRD) and superconducting quantum interference device magnetization measurements.

## 3. Results and discussion

### 3.1. BaTiO<sub>3</sub>

Fig. 1 (top) shows a magnetization versus field ( $M-H$ ) plot at 10 K from BaTiO<sub>3</sub> implanted with 5 at.% Mn, while the difference in magnetization between field-cooled and zero field-cooled conditions (at 1000 Oe) is shown at the bottom of the Figure. Qualitatively similar results were obtained for 3 at.% Mn samples, with coercivities of ~600 G at 10 K and ~400 G at 100 K. The  $M-T$  plots do not show a classical Curie–Weiss shape, but current theories suggest the shape of these plots is controlled by disorder in the sample and any shape from concave to linear to convex is possible [28]. Note that the net magnetization reaches zero at approximately room temperature. XRD showed no evidence of other phases present in the implanted samples.

Co implantation also produced signatures of ferromagnetism, as shown in Fig. 2. The coercivities were again of order a few hundred Gauss at 300 K for both 3 and 5 at.% Co concentrations, while the  $M-T$  plot showed an almost linear dependence on temperature. XRD data showed no evidence of secondary phase

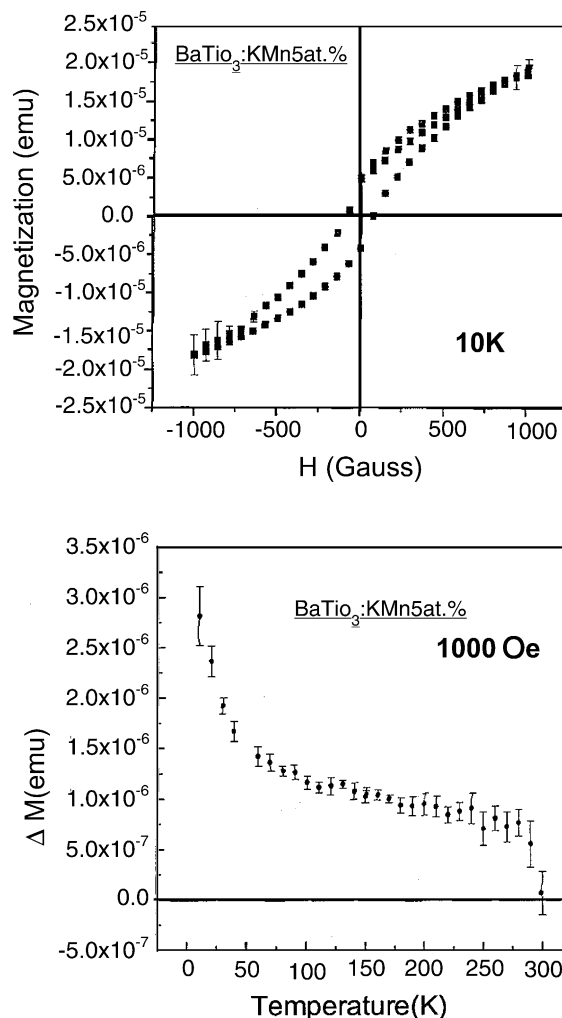


Fig. 1. Magnetization loop at 10 K for field applied perpendicular to the plane of a BaTiO<sub>3</sub> sample implanted with 5 at.% Mn (top), and temperature dependence of the difference of field-cooled and zero field-cooled magnetization at a field of 1000 Oe (bottom).

formation or the presence of Co clusters that would influence the magnetic properties of these samples.

The ab-initio total energy calculations for BaTiO<sub>3</sub> doped with all the 3d transition metals from Sc to Cu indicate that Mn, Fe, Cr and Co are the most promising candidates for achieving ferromagnetism in conducting samples. While these calculations should be used as a guide only due to hybridization effects and the high transition metal concentrations assumed, they are in relatively good agreement with our initial experimental data. The mechanism for the observed ferromagnetism is still not clear and may be due to bound magnetic polarons [28,29] or the carrier-induced magnetism inherent in the Zener mechanism [20].

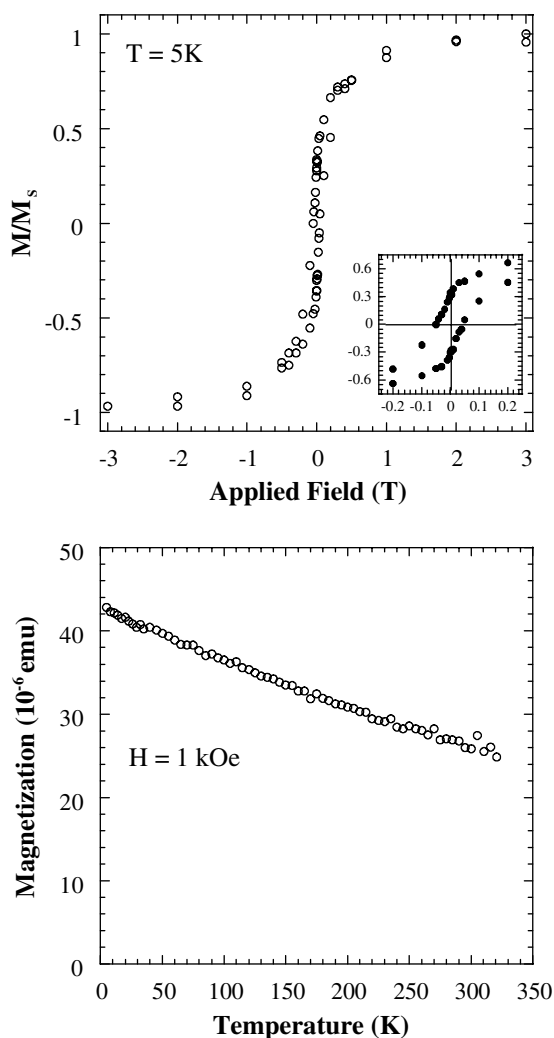


Fig. 2. Magnetization loop at 5 K for field applied perpendicular to the plane of a BaTiO<sub>3</sub> sample implanted with 5 at.% Co (top), and temperature dependence of the magnetization at a field of 1 kOe for a sample implanted with 3 at.% Co (bottom).

### 3.2. SrTiO<sub>3</sub>

While SrTiO<sub>3</sub> samples with 5 at.% Mn showed paramagnetic behavior, at the 3 at.% Mn concentration clear signatures of ferromagnetism near 300 K were evident in the *M*–*H* and *M*–*T* plots (Fig. 3). These results would be consistent with the Dietl et al. [20] model in which the net magnetization is given by the difference between the carrier-mediated ferromagnetism and the antiferromagnetic direct interactions between Mn<sup>+</sup> ions. In this model, the Curie temperature *T*<sub>C</sub> can be represented

$$T_C = \frac{\chi_{\text{eff}} N_O S(S+1) \beta^{\otimes} A_F \rho_s |\psi|^2}{12k_B} - T_{\text{AF}}$$

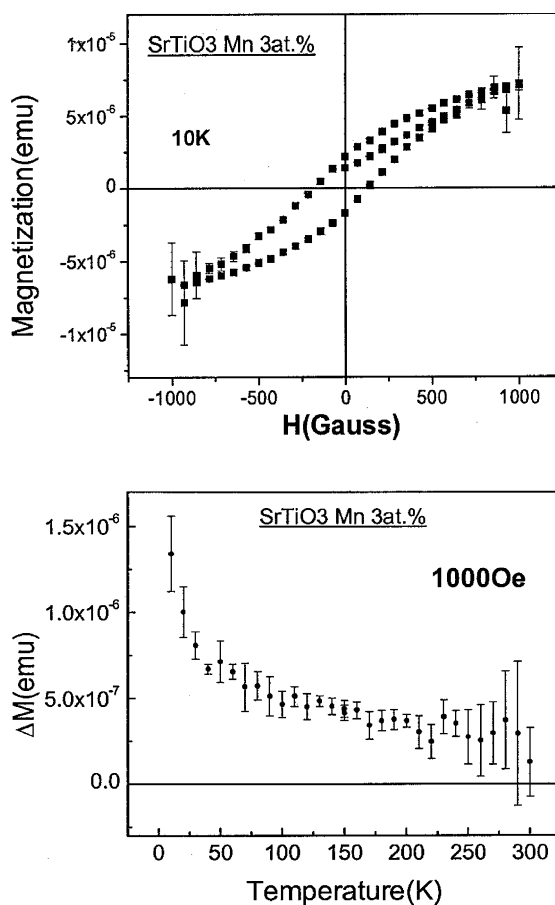


Fig. 3. Magnetization loop at 10 K for field applied perpendicular to the plane of a SrTiO<sub>3</sub> sample implanted with 3 at.% Mn (top), and temperature dependence of the difference of field-cooled and zero field-cooled magnetization at a field of 500 Oe (bottom).

where  $\chi_{\text{eff}} N_O$  is the Mn concentration,  $\beta$  is the strength of the interaction between the Mn and the carriers,  $\rho$  is proportional to the effective mass of the carriers and  $T_{\text{AF}}$  takes into account antiferromagnetic Mn–Mn interactions. Thus, the *T*<sub>C</sub> can decrease at high Mn concentrations due to the increase in the latter contribution to the magnetization.

In the case of Co implantation, hysteresis was observed at 300 K for both the 3 and 5 at.% concentrations and the *M*–*T* showed the opposite curvature to the normal Brillouin-like dependence. In the disorder model [28,29], holes are only allowed to hop between transition metal acceptor sites and the interaction between the holes and the magnetic ions is of the antiferromagnetic Heisenberg exchange type. The shape of the *M*–*T* plot is then determined by the wide distribution of exchange couplings because of disorder because some Mn atoms do not order until lower temperatures. This unusual

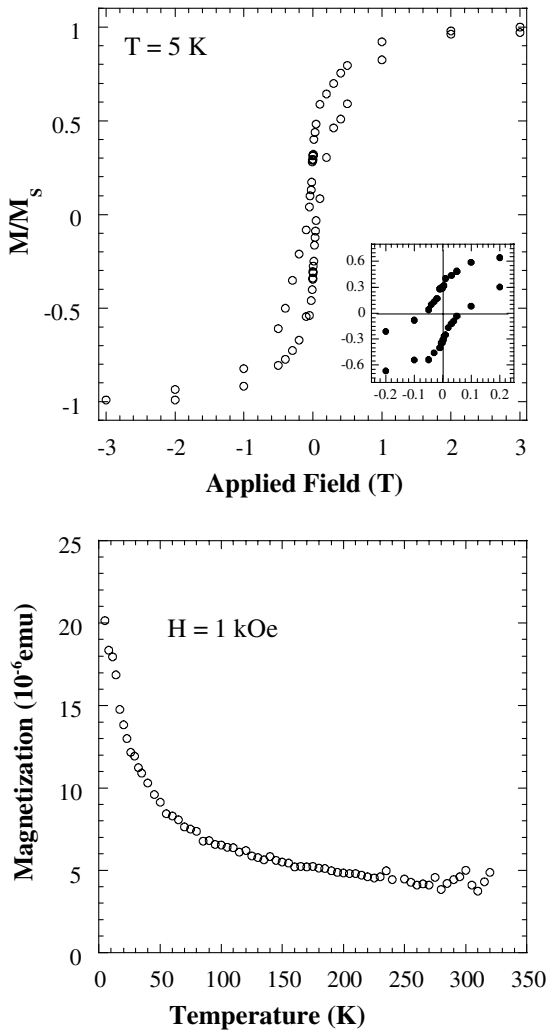


Fig. 4. Magnetization loop at 300 K for field applied perpendicular to the plane of a  $\text{SrTiO}_3$  sample implanted with 5 at.% Co (top), and temperature dependence of the magnetization at a field of 1 kOe for a sample implanted with 3 at.% Co (bottom).

magnetization is in good agreement with our experimental data, as shown in Fig. 4. Another interesting feature of this theory is that with increasing randomness, the  $T_C$  increases and the saturation value of the magnetization is decreased [28,29]. Within the same model, if the carrier concentration is increased, the change of the magnetization becomes more Brillouin-like because the width of the exchange interaction decreases [30–33].

### 3.3. $\text{KTaO}_3$

Fig. 5 shows the  $M-H$  (top) and  $M-T$  (bottom) plots from the material implanted with 3 at.% Mn. Quanti-

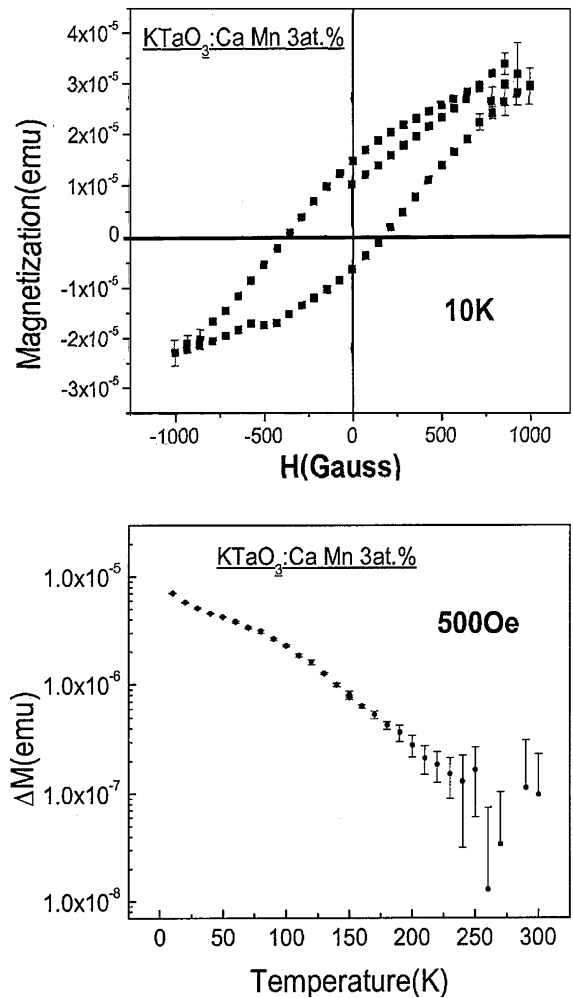


Fig. 5. Magnetization loop at 10 K for field applied perpendicular to the plane of a  $\text{KTaO}_3$  sample implanted with 3 at.% Mn (top), and temperature dependence of the difference in field-cooled and zero field-cooled magnetization at a field of 500 Oe (bottom).

tatively similar results were obtained for the 5 at.% condition. The magnetic ordering is present to  $\sim 250\text{ K}$  and once again no additional peaks were observed in the XRD spectra from the samples.

The Co implantation produced higher magnetic ordering temperatures than for Mn, with hysteresis loops observed at 300 K for both the 3 and 5 at.% concentrations and magnetization extending to at least the same temperature (Fig. 6). At present there is not published data for the theoretically predicted properties of transition metal-doped  $\text{KtZO}_3$ , so our data serves as a starting point for understanding the magnetic properties.

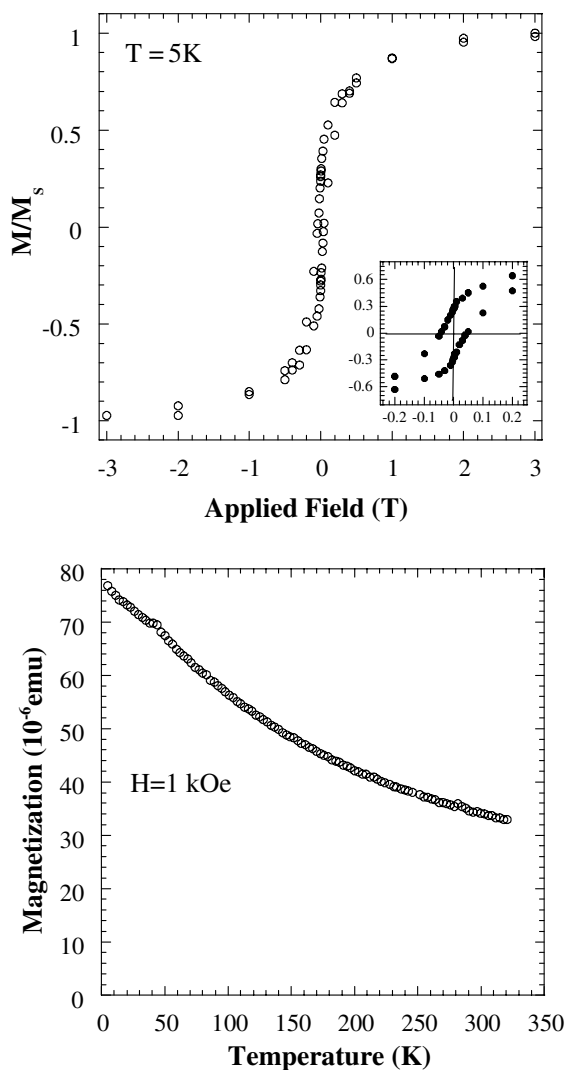


Fig. 6. Magnetization loop at 300 K for field applied perpendicular to the plane of a  $\text{KTaO}_3$  sample implanted with 3 at.% Co (top), and temperature dependence of the magnetization at a field of 1 kOe (bottom).

#### 4. Summary and conclusion

Three different oxide perovskites,  $\text{BaTiO}_3$ ,  $\text{SrTiO}_3$  and  $\text{KTaO}_3$ , show promising magnetic behavior when doped with Mn or Co by direct ion implantation. In each magnetic ordering was observed at  $\geq 250$  K and above room temperature in some cases. The magnetization has the opposite occurrence to the usual Brillouin-like dependence on temperature, as is predicted by a model that takes into account the effects of disorder in dilute magnetic systems [28–33]. In this model the ferromagnetism may arise from the interaction between magnetic polarons in the case of either

low carrier density or equivalently, strong carrier localization.

#### Acknowledgements

The work at SNU was partially supported by KOSEF and Samsung Electronics Endowment through SCSMR. The work at UF is partially supported by NSF (DMR-0101856 and DMR-0101438) and by ARO.

#### References

- [1] von Helmlolt R, Lecker J, Holzapfel B, Schultz L, Samwer K. *Phys Rev Lett* 1993;71:2331.
- [2] McCormack M, Jin S, Tiefel TH, Fleming RM, Phillips JM, Ramesh R. *Appl Phys Lett* 1994;64:3045.
- [3] Jin S, Tiefel TH, McCormack M, Fastnacht RA, Ramesh R, Chen LH. *Science* 1994;264:413.
- [4] Sun JZ, Krusin-Elbaum L, Gupta A, Xiao G, Duncombe PR, Parkin SSP. *IBM J Res Develop* 1998;42:89.
- [5] Coey JMD, Viret M, von Molnar S. *Adv Phys* 1999;48:167.
- [6] Ramirez AP. *J Phys C Condens Matter* 1997;9:8171.
- [7] Wolf SA, Awschalom DD, Buhrman RA, Daughton JM, von Molnar S, Roukes ML, et al. *Science* 2001;294:1488.
- [8] Ohno H, Matsukura F, Ohno Y. *JSAP Int* 2002;5:4.
- [9] Sonoda S, Shimizu S, Sasaki T, Yamamoto Y, Hori H. *J Cryst Growth* 2002;237-239:1358.
- [10] Thaler GT, Overberg ME, Gila B, Frazier R, Abernathy CR, Pearton SJ, et al. *Appl Phys Lett* 2002;80:3964.
- [11] Reed ML, El-Masry NA, Stadelmaier HH, Rittums ME, Reed NJ, Parker CA, et al. *Appl Phys Lett* 2001;79:3473.
- [12] Overberg ME, Gila BP, Thaler GT, Abernathy CR, Pearton SJ, Theodoropoulou NA, et al. *J Vac Sci Technol B* 2002;20:969.
- [13] Theodoropoulou NA, Hebard AF, Chu SNG, Overberg ME, Abernathy CR, Pearton SJ, et al. *J Appl Phys* 2002;91:7499.
- [14] Jung SW, An S-J, Yi G-C, Jung CU, Lee S-I, Cho S. *Appl Phys Lett* 2002;80:4561.
- [15] Ueda K, Tabota H, Kawai T. *Appl Phys Lett* 2001;79:988.
- [16] Chambers SA, Thevuthasan S, Farrow RFC, Marks RF, Thiele JU, Folks L, et al. *Appl Phys Lett* 2001;79:3467.
- [17] Matsumoto Y, Murakami M, Shono T, Hasegawa T, Kukomura T, Kawasaki Metal. *Science* 2001;291:854.
- [18] Sato K, Katayama-Yoshida H. *Jap J Appl Phys* 2001;40:L334; *Mat Res Soc Symp Proc* 2001;666:F4.6.1.
- [19] Sato K, Katayama-Yoshida H. *Physica E* 2001;10:251 *Jap J Appl Phys* 2000;39:L555.
- [20] Dietl T, Ohno H, Matsukura F, Cibert J, Ferrand D. *Science* 2000;287:1019.
- [21] Nakagawa H, Katayama-Yoshida H. *Jap J Appl Phys* 2001;40:L1355.
- [22] Jin Z, Hasegawa K, Fukumura T, Yoo YZ, Hasegawa T, Koinuma H, et al. *Physica E* 2001;10:256.
- [23] Wakano T, Fujimura N, Morinaga Y, Abe N, Ashida A, Ito T. *Physica E* 2001;10:260.
- [24] Tiwari A, Jin C, Kuit A, Kumar D, Muth JF, Narayan J. *Solid-State Comm* 2002;121:371.

- [25] Fukumura T, Jin Z, Kawasaki M, Shono T, Hasegawa T, Koinuma H. *Appl Phys Lett* 2001;78:958.
- [26] Kimura H, Fukumura T, Kawasaki M, Inaba K, Hasegawa T, Koinuma H. *Appl Phys Lett* 2002;80:94.
- [27] Zhang J, Tanaka H, Kanai T. *Appl Phys Lett* 2002;80:4378.
- [28] Berciu M, Bhatt RN. *Phys Rev B* 2001;65:107203.
- [29] Angelescu DE, Bhatt RN. *Phys Rev B* 2002;65:075211.
- [30] Berciu M, Bhatt RN. *Physica B* 2002;312/313:815.
- [31] Durst AC, Bhatt RN, Wolff PA. *Phys Rev B* 2002;65:235205.
- [32] Bhatt RN, Berciu M, Kennett MD, Wan X. *J Supercond Incorporating Novel Magn* 2002;15:71.
- [33] Chudnovskiy AL, Pfannkude D. *Phys Rev B* 2002;65:165216.